

PROCEEDINGS OF SPIE

[SPIEDigitallibrary.org/conference-proceedings-of-spie](https://www.spiedigitallibrary.org/conference-proceedings-of-spie)

Emerging developments in tomographic imaging with hard x-rays

Müller, Bert

Bert Müller, "Emerging developments in tomographic imaging with hard x-rays," Proc. SPIE 11840, Developments in X-Ray Tomography XIII, 1184004 (16 November 2021); doi: 10.1117/12.2595054

SPIE.

Event: SPIE Optical Engineering + Applications, 2021, San Diego, California, United States

Emerging developments in tomographic imaging with hard X-rays

Bert Müller^{*a,b}

^aBiomaterials Science Center, Department of Biomedical Engineering, University of Basel, 4123 Allschwil, Switzerland; ^bBiomaterials Science Center, Department of Clinical Research, University Hospital Basel, 4031 Basel, Switzerland

ABSTRACT

This year, we celebrate the 125th anniversary of medical imaging based on RÖNTGEN's discovery. Human hands with a metallic ring have been replicated numerous times. The early radiographs show impressive details on the bony structure. Thanks to tomographic imaging, the advanced X-ray instrumentation, the sophisticated algorithms of reconstruction and data evaluation as well as the preparation beyond the well-established staining we can make visible the micro- and nanostructures of the bone with its surrounding tissues with unequalled details, just to mention one example. This paper summarizes selected key aspects of the contributions in the 13th volume on *Developments in X-ray Tomography*, which have emerged over the last two years.

Keywords: Computed tomography, phase tomography, microtomography, nanotomography, synchrotron radiation, image analysis, artificial intelligence, multimodal imaging.

1. INTRODUCTION

High-resolution hard X-ray tomography using laboratory- and synchrotron radiation-based sources enables us to three-dimensionally visualize a wide variety of objects without physical slicing. The three-dimensional data represent physical quantities related to the local X-ray absorption coefficients, the local electron densities and their combination. Currently, the laboratory-based instruments, which have been mainly employed the absorption contrast, are also capable using the phase-contrast mode. This mode can, for example, be successfully used to image physically soft animal and human tissues *post mortem* or from biopsies without the necessity of staining.

A microtomography experiment requires the instrument consisting of source, high-precision manipulator with rotation stage and detection unit, which fits the imaging of the object of interest. The preparation and handling of the objects is often underestimated, as impressively demonstrated by the plenary talk "A mummy's secret" and the related paper by Fellow of SPIE Stuart R. Stock [1].

The acquired data series of current tomograms reached a size in the TB-range or went even beyond. Manual evaluation is, therefore, not meaningful anymore. Powerful algorithms are required to reconstruct the tomographic data, to reduce artifacts and noise, to identify features of interest, to quantify them on the basis of advanced segmentation tools, and to register them to study time-dependent phenomena. The plenary talk by the Fellow of SPIE Ge Wang entitled "X-ray imaging meets deep learning" has given insights into the currently available possibilities [2].

Alternatives to conventional attenuation-based tomography include phase tomography, spectral imaging and three-dimensional reciprocal-space techniques. They are based on advances in X-ray sources and detector technologies such as liquid metal sources, compact light sources, and photon-counting spectral detectors. The valid comparisons of the CT-systems is object-dependent but includes the quantitative characterization of sources, sample manipulators, detectors and the related image-quality assessment. The impact of the filters implemented in reconstruction and artifact compensation is often underestimated. The gain of appropriate filter selection, however, is convincing. It is often a prerequisite to seriously apply automatic procedures of feature extraction and registration with other two- or three-dimensional datasets for multimodal imaging.

*bert.mueller@unibas.ch; phone +41 61 207 5430; fax 41 61 207 5499; www.bmc.unibas.ch

The current proceedings volume contains 43 contributions in total. SPIE's Digital Library lists 38 contributions with both presentation and paper, one contribution with paper only, and four presentation-only contributions. The authors of these four presentations had reasonable arguments for the missing proceedings paper; one can find the same or similar results in the literature, as detailed below. Figure 1 shows a comparison of the contributions with the previous volumes. The impact of the COVID 19 pandemic is hardly visible, although many research activities have been affected and traveling was seriously restricted.

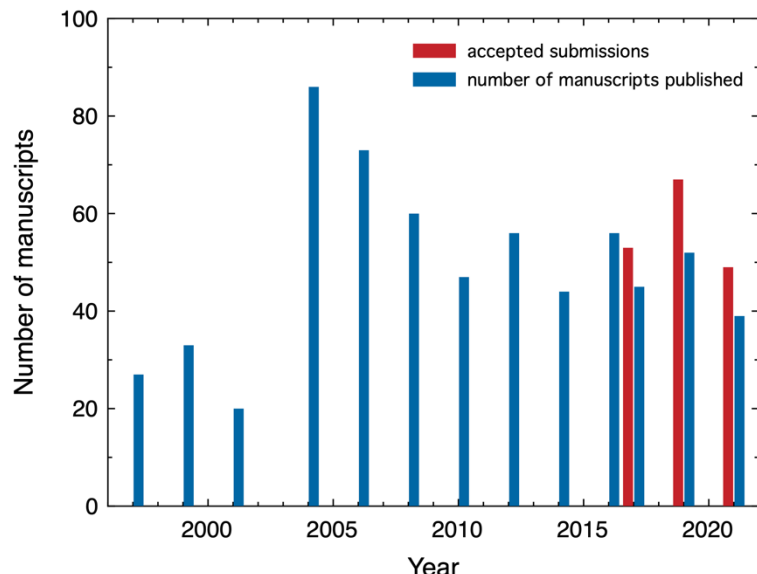


Figure 1. In 1997, the conference series on *Developments in X-ray tomography* was initiated by the experimental physicist and pioneer in the field Ulrich Bonse, Emeritus of Physics, former Vice Rector, and one of the two Honorary Senators at the University of Dortmund, Germany. He successfully chaired the conference for five times. Subsequently, Stuart R. Stock, Research Professor of Cell and Developmental Biology at Feinberg School of Medicine, Northwestern University, Chicago, with over forty years of experience in the field, chaired the conference for five times as well. In the years 2017, 2019 and 2021, Ge Wang and I have had the privilege chairing the conferences. This year, the number of in-person presentations was low because of the travel restrictions. Nonetheless, 40 talks and three posters were presented. Only eight accepted contributions were withdrawn.

2. EVOLUTION OF INSTRUMENTATION FOR X-RAY TOMOGRAPHY

A Chinese research team showcased a two-dimensional array field-emission source, termed flat-panel source [3]. Although the current flat-panel source is in its infancy, the simulations and preliminary experimental data are promising.

Sandia National Laboratories developed a multi-metal patterned anode for tomography with improved spatial resolution and signal-to-noise ratio at photon energies of the absorption lines from the anode materials [4]. Simulations showed that the patterned design of the anode reduced the total focal spot size associated with improved spatial resolution.

A research team from Japan developed a structured anode X-ray source for grating interferometry at a design photon energy of 82 keV [5]. The impressive performance of this source implemented in an inverse Tabot-Lau interferometer was demonstrated for the imaging of an interior of a steel screw. In addition, the authors presented images of a freshly charged and discharged AA alkaline battery using the representations in attenuation, refraction and scattering modes and discussed the structural changes by discharging.

Conventional electron-impact sources possess a limited brightness, monochromaticity, tunability and coherence with respect to synchrotron radiation facilities. These facilities, however, have limited access. An inverse Compton scattering X-ray source bridges this gap. It works by colliding a high-power laser beam with a relativistic electron beam to generate

back-scattered photons in the X-ray regime. B. Hornberger and J. Kasahara presented such a system for tomographic imaging – the Munich Light Source [6].

Optical elements for X rays have serious limitations. A Russian team evaluated boron carbide for refractive optics, because this material could combine high refractive ability with high X-ray transmission [7]. They showed how far tomographic imaging could be used to improve the manufacturing towards X-ray refractive optical elements.

Synchrotron radiation is known to provide a broad spectrum of hard X rays. The frequently used undulator sources can create a filtered broadband illumination for fast grating-based tomography, as shown S. Marathe and coworkers active at the beamline I13-2, Diamond Light Source, Dicot, UK [8]. The setup - filtered pink-beam, single grating X-ray Talbot interferometer - had been used to image a bee head in three contrast modes. For radiographic imaging, they reached an acquisition rate of 17 Hz applying 50 ms exposure time. The possibilities of this beamline was also demonstrated by C. Rau *et al.* [9]. They demonstrated fast tomographic imaging down to the nanometer scale. The robotic sample changer allows for tomography of up to 300 samples per day. The planned 2027 Diamond upgrade will further increase the performance of this imaging beamline.

Beamtime at synchrotron radiation facilities is easily accessible for interested applicants from industry. M. Thiry and team gave insight into the possibilities at the beamlines P05 and P07, storage ring PETRA III of the Deutsches Elektronen-Synchrotron DESY, Hamburg, Germany [10]. The two tomography setups, operated by the Helmholtz-Zentrum Hereon, allow for measurements at photon energies between 10 and 200 keV. The authors provided examples from space industry, metal powder-based additive manufacturing, and metrology of strongly X-ray absorbing hafnium in a silver matrix. The same tomography stations were used to image murine and human kidneys [11]. M. Riedel *et al.* developed a speckle-based approach for optimized phase retrieval at 2 μ m resolution. F. Beckmann and coworkers gave an overview on hierarchical tomographic imaging at these beamlines, which became more stable in operation with improved user-friendliness [12]. Thus, the community can submit beamtime proposals for a wide range of applications, see below.

Recently, laboratory-based X-ray fluorescence computed tomography implementing nanometer-sized metallic contrast agents has reached maturity and may be even used for preclinical imaging *in vivo* [13]. The authors simultaneously showed Mo, Ru, and Rh nanoparticles in a sacrificed mouse [14].

M. Andrew and coworkers presented automated training of deep learning networks for the X-ray reconstruction with the aim to reduce noise and sparse sampling artefacts [15]. They also showed a technique for the removal of propagation phase contrast phenomena at high-resolution data acquired with rather low acceleration voltages. This removal has uncovered the inherent reconstructed material contrast for more effective denoising and segmentation, as impressively demonstrated for a pharmaceutical powder [15].

3. DEVELOPMENTS OF ALGORITHMS FOR TOMOGRAPHIC IMAGING AND ANALYSES

3.1 Advanced reconstruction algorithms

For *in vivo* CT imaging the employed radiation dose determines the image quality. It should be minimized without compromising the image quality. Therefore, low-dose CT, often associated with noisy images and weak contrast, has been a hot topic. Q. Zhang *et al.* [16] successfully proposed the learned descent algorithm with line search for such a low-dose CT reconstruction. This algorithm yields an interpretable neural network architecture, where the regularization parameterized as multilayer perception is explicitly integrated into the iterative scheme and learned during training process. The algorithm retains convergence guarantee, while achieving improved efficiency and accuracy in low-dose CT image reconstruction.

M.G. Grewar *et al.* [17] described an approach to quadratically expanding loglikelihood under a general noise model. Based on simulation, they showed the successful implementation to maximize likelihood under mixed Poisson-Gaussian models for a range of CT imaging systems.

Streak artifacts originate from highly X-ray absorbing parts including metal implants in human tissue. C. Niu *et al.* [18] enhanced the existing deep learning-based methods restricted to a single CT number window to multiple such windows. Experimental results demonstrate the strength of the software to reduce such metal artifacts in clinical CT images.

M. Li *et al.* [19] introduced a deep-learning framework for interior CT. They trained a network on low-resolution data for high-resolution interior reconstruction and obtained decent performance in realistic simulations. The focus was on a temporal bone imaging with a region of interest at predefined locations in the human head. The approach, however, might be beneficial for a range of other applications, including hierarchical imaging, given its low cost of training data preparation. An experimental proof is still pending.

Details within CT data such as micro-anatomical features are often difficult to access and visualize. C. Tanner *et al.* [20] presented an automatic procedure to uncover the 3 μm -thin annual layers in human tooth cementum. To avoid physical slicing of the unique teeth, the projections were stitched before reconstructing slices of $1.3 \cdot 10^8$ voxels. To identify high-contrast annual layers, the team considered projections orthogonal to the layers by optimizing the image contrast through tilting.

Beam hardening correction algorithms have been improved over decades. G. Davis has proposed an extension for polychromatic radiation and a hierarchically organized phantom, *i.e.* a liquid-immersed tooth [21]. Adjusting the model parameters, the accuracy in measuring mineral concentration was substantially improved.

3.2 Propagation-based or spectrally sensitive reconstruction

Propagation-based CT avoids optical elements in the imaging system. Phase-contrast effects are detected via intensity variations on the detection plane. Suitable phase-retrieval analysis of the recorded data is necessary for the extraction of quantities. Within a short communication, F. Schaff *et al.* [22] described the combination of spectral X-ray and propagation-based imaging for material decomposition.

C. Wiedeman *et al.* [23] proposed a deep learning-based solution for the simultaneous scatter and attenuation image reconstruction from single-view, multi-energy scatter data. Currently, this fundamental approach cannot be applied, because it requires better monochromatized X-ray beams and improved detector energy resolution. It is a valuable proposal, which needs further developments including the compensation for multi-scattering events.

The sources of lab-based CT systems generate polychromatic X-rays. The resulted tomographic data can only be related to quantitative absorption values after appropriate calibration. Q. Yang *et al.* [24] applied the ALVAREZ-MACOVSKI equation in iterative reconstruction to model the local X-ray attenuation coefficients. The preliminary results were promising, as another perspective from the iterative reconstruction side for the quantitative tomogram interpretation has been generated.

R. Ueda *et al.* [25] coupled a microscope with a Lau interferometer for phase tomography, which is especially advantageous in tomographic imaging of materials with low atomic numbers. To prevent discontinuous phase jumps in the twin-phase image, which propagates artifacts over the entire image through the deconvolution, the authors presented the three-wave interference model. The approach gave additional insight into the validity of the conventional two-beam model and broadened the applicability of the microscope developed.

The paper of S.J. Alloo *et al.* [26] provides a comprehensive overview on CT imaging modalities with a focus on speckle-based X-ray dark-field tomography. Contrary to several existing approaches, the authors also included the attenuation of the object - pieces of wood. Profiles display the differences between the projected thickness, the phase-object and attenuating-object signal. The reconstructions were based on six sets of images acquired at pre-selected transverse positions of the speckle mask, with a significant application potential.

3.3 Image analysis

CT images reveal the geometry of the object of interest. R. Ammann *et al.* [27] utilized this capacity to measure the local thicknesses of optically transparent and removable teeth braces fabricated via thermoforming at preselected process

temperatures. These aligners possess a complex morphology. As a result, gaps between teeth and braces cannot be avoided. The quantitative evaluation of the gaps by the automatic CT data analysis allowed for an optimization of the fabrication procedure for a given starting material.

V. Cooley *et al.* [28] focused on the challenges in segmenting teeth in mice. Intensity-based segmentation methods cannot handle the mineral gradients, especially those in forming enamel in the continuously growing incisors. The authors, therefore, employed convolutional neural networks. A network for wild-type hemimandibles was trained on 1,600 images with an edge length of 128 voxels. The network underperformed when applied to test slices from two mutant jaws – not wild type, but performance was noticeably improved by incorporating training data from the mutants. This research promised to accelerate the segmentation of large amounts of CT images generated for mutant lines.

Hard X-ray tomography has been constantly used for non-destructive evaluation. E. Lindgren and C. Zach [29] gave a recent example. They reported a comprehensive study on analysis of products based on additive manufacturing. Publicly available CT-data of additively manufactured metals were processed with deep neural networks. The authors showed that incorporating modeled X-ray noise during training can reduce artifacts in the generated imperfection indications and improved the out-of-distribution detector performance.

4. CUTTING-EDGE APPLICATIONS OF COMPUTED TOMOGRAPHY

4.1 Computed tomography of unique objects

Unique objects with the size of a human skull are generally imaged by means of laboratory-based systems, because most of the currently available synchrotron radiation-based CT-systems only possess a field of view in the millimeter range. G. Schulz *et al.* [30] investigated such an object, namely a prehistoric skull of a five-year-old child. The obtained tomography data underwent a three-dimensional distance transform to extract the skull thickness distribution. This thickness distribution seems be of interest for the diagnosis of relevant diseases. The irregularities in the present case indicate an intracranial pressure raise.

A. Nelson [31] presented an abstract of the history of X-ray imaging mummies. He elucidated the interdisciplinary character of such an endeavor and the lack of standardization. The study predicted future developments in computed tomography of mummies on the basis of radiological investigations back more than a century. The author requested for further innovations in tomographic imaging of mummies.

J. Romell *et al.* [32] presented a high-resolution tomography study of the buff-tailed bumblebee's eye. The data obtained with a liquid-metal X-ray source showed a spatial resolution of 200 to 300 nm and are, therefore, comparable to light and electron microscopies as well as synchrotron radiation-based data [33]. Surprisingly, the non-stained samples gave rise to better image quality than the stained ones. The cornea, the crystalline cones and the pigments were clearly resolved [33].

4.2 Medically relevant tomographic imaging: Hard tissues

D. Mills and A. Boyde [34] performed an imaging study correlating light microscopy and conventional hard X-ray tomography with a voxel size of 20 μm . For the efficient tomography experiments, they built a 25 mm stack of glass slides, where 15 unique conventional microscopy slices from bone and calcified cartilage as well as from dentine, enamel, and cementum were sandwiched between the microscopy slides and the cover slips. The tomography images exhibit the commonly known microanatomical features with their anisotropy, especially prominent for the teeth slices of the selected animals.

S.R. Stock *et al.* [35] investigated a complete abdominal vertebra of a blue shark using conventional microtomography and energy dispersive diffraction (EDD) with polychromatic synchrotron radiation. In addition, they cut another shark vertebrae into sections parallel to the vertebral column's axis to obtain slices less than 1 mm thick and squares about 2.5 mm cross-sections for fluorescence mapping and synchrotron radiation-based tomography, respectively. The authors have shown that the shark centrum consists of a double cone structure supported by four wedges. Whereas the bioapatite

within the cone wall is oriented with its *c*-axes lateral, *i.e.* perpendicular to the axis of the backbone, the bioapatite within the wedges is oriented with its *c*-axes axial.

K. Iskhakova *et al.* [36] presented diffraction tomography experiments on sheep tibia around a Mg-Zn-Ca implant. After six weeks of healing, the partially degraded implant with surrounding bone was explanted. Whereas the hydroxyapatite's *d*-spacing was not affected by the resorbable bone implant, the crystal sizes were reduced at 1.5 mm compared to 3 mm distance, a phenomenon probably caused by the degradation products incorporated into the bone remodeling processes.

4.3 Medically relevant tomographic imaging: Soft tissues

M. Eckermann *et al.* [37] pushed tomographic imaging up to its limits in order to visualize murine corpus callosum tissue, which is rich in myelinated nerve fibers. By the combination with focused ion-beam scanning electron microscopy, the authors established a correlative imaging work flow for stained and embedded brain tissue.

High-resolution tomography experiments on non-stained human or animal tissues are often performed after paraffin embedding, a preparation procedure well known from histology. G. Rodgers *et al.* [38] three-dimensionally visualized a mouse brain with voxel sizes of 3.1 and 0.7 μm , respectively, at the intermediate preparation steps of formalin fixation and paraffin embedding. Ethanol dehydration and paraffin embedding are preferable for virtual histology thanks to improved contrast, though both lead to locally varying volume changes relative to the formalin-fixated state [39, 40]. Ethanol dehydration enhanced white matter contrast and allowed segmenting fiber tracts. The paraffin-embedded brain provided superior contrast between the cerebellum layers.

W. Twengström *et al.* [41] also performed a virtual histology study of paraffin-embedded tissue. The non-stained tissues of the tomography study to access the tumor resection margins were human pancreatic neuroendocrine tumors, liver intrahepatic cholangiocarcinoma, and benign pancreatic serous cystic neoplasm. Comparing the tomography data with histology, the authors observed the tumors with distinct and sharp edges at about 10 μm resolution. Together with the assisting histological landmarks, the approach allowed for precise resection margin assessment. The authors claimed that the combination of a liquid-metal jet microfocus source and a scintillator-coated CMOS detector enabled laboratory-based phase tomography for intra-operative three-dimensional virtual histology.

An alternative method for intraoperative imaging was presented by O. Roche I Morgó *et al.* [42]. The authors introduced cycloidal computed tomography and claimed that the method was comparable to phase tomography concerning contrast and spatial resolution as well as kept the scan times short thanks to an effective under-sampling. Preliminary results were obtained for a tissue-engineered esophagus, *i.e.* a cell-seeded pig-derived acellular scaffold, and formalin-fixated, human, resected, tumor-bearing breast tissue of centimeter size.

Breast mastectomy imaging also was in the focus of a comprehensive synchrotron radiation-based tomography study of B.D. Arhatari *et al.* [43]. Using eleven fresh full-breast mastectomy samples, the authors compared absorption- and phase-contrast acquisitions changing the sample-to-detector distance from 0.19 to 6.00 m and keeping the mean glandular dose at 4 mGy each. Eight breast samples contained cancer lesions; two cancer-free samples originated from prophylactic surgery and one from a patient after completing chemotherapy. For these samples with a wide variation in dimension, density and composition, the authors could demonstrate the advantages of propagation-based phase tomography with respect to the absorption-based approach qualitatively, *i.e.* by the visual inspection of trained radiologists, and quantitatively via the quotient of signal-to-noise ratio and spatial resolution.

5. AWARDED CONTRIBUTIONS

The program committee members selected three best papers from 14 finalists. They show the diversity ranging from the advancements in instrumentation via the developments of algorithms to the wide-spread applications as well as relate to geographic origin, gender, and level of career.

5.1 State of the art and recent advances in X-ray speckle-based phase-contrast imaging

M.-C. Zdora *et al.* [44] presented an overview on speckle-based imaging using X-ray beams. This phase-contrast method is simple, cheap, and robust. Its sensitivity allowed detecting minute density modulations, as exemplarily demonstrated for murine soft tissue and a sample from geology. The authors highlighted the advantages of the unified modulated pattern analysis. Finally, the authors successfully acquired speckle-based projection images by means of a laboratory-based setup. Additional adaptations on the X-ray spot size, the photon energy spectrum, the detection unit, *etc.* are necessary to become compatible with tomography at reasonable acquisition times.

5.2 Dual-domain reconstruction network for sparse-view computed tomography

Y. Zhang *et al.* [45] introduced an approach to reduce artifacts and to preserve details within tomography data especially for clinical applications. The research team combined the image and projection domains for the sparse-view problem. The model integrated two parallel and interactive subnetworks to perform image restoration and sinogram inpainting operations on both domains simultaneously to fully explore the relation between projection data and reconstructed images. The approach is highly welcomed to reduce radiation-induced cancer, to extend the diagnostic capabilities of X-ray computed tomography, and to enable treatment planning on the basis of the tomographic data.

5.3 Laboratory-based phase and absorption tomography for microimaging of annual layers in human tooth cementum, paraffin-embedded nerve and zebrafish embryo

A. Migga *et al.* [46] selected three medically relevant samples to compare the performance of three next-generation laboratory-based tomography systems. Using the comparison with a few years old conventional μ CT and with the gold standard synchrotron radiation-based tomography systems, the authors could demonstrate the impressive advances in laboratory-based tomography. First, the 3 μ m-thin annual layers in human tooth cementum were made visible. Second, the biological cells within a zebrafish larva were uncovered. Third, the spiral nature of the myelin sheaths in a porcine nerve was evaluated and presented by videos. Thanks to these advances, propagation-based phase-contrast microtomography is no longer reserved for synchrotron radiation facilities.

6. PROCEEDINGS OF SPIE VOLUME 11840: BARGAIN BOX FOR THE INTERDISCIPLINARY COMMUNITY ACTIVE IN TOMOGRAPHY

SPIE's proceedings volumes on *Developments in X-Ray Tomography* contain a wealth of information. Established in 1997 by an expert team around the pioneer U. Bonse, it is known as the longest running non-clinical tomography conference. The submitted abstracts are critically vetted by the conference chairs in close coordination with the members of the program committee before acceptance. Much more important are the proceedings papers with a mean length of 10.6 pages for the current volume and 9.9 pages for volume 11113 from 2019 just to mention the last two conference proceedings. With 30,000 to 40,000 characters the paper's content substantially exceeds the typical extended abstracts or papers of many conferences. Most importantly, the authors have integrated the professional feedback from the scientific discussions during the conference and reports from the committee members as reviewers, adapted their manuscripts accordingly for formal publication in our proceedings volume. This fact has been also the reason, why the proceedings papers from this conference series are much more frequently cited than the ones of some other SPIE conference proceeding papers. The proceedings volumes on *Developments in X-Ray Tomography* have been regarded as a bargain box for the interdisciplinary community working in the fascinating area of hard X-ray tomography. It also serves as a periodic snapshot and central place where papers from many disciplines - focusing on hard X-ray tomography - mingle.

ACKNOWLEDGEMENT

The author gratefully acknowledges the valuable input of Stuart R. Stock and Ge Wang.

REFERENCES

- [1] Stock, S. R., "A mummy's secrets," *Proc. SPIE* **11840**, 1184003 (2021).
- [2] Wang, G., "X-ray imaging meets deep learning," *Proc. SPIE* **11840**, 1184002 (2021).
- [3] Duan, J., Wang, T., Li, Y., and Mou, X., "A high-order prior for overlapped projections in the real flat-panel x-ray source imaging system," *Proc. SPIE* **11840**, 118401B (2021).
- [4] Dalton, G., Collins, N., Clifford, J., Kemp, E., Limpanukorn, B., and Jimenez, E. S., "Monte-Carlo modeling and design of a high-resolution hyperspectral computed tomography system with multi-material patterned anodes for material identification applications," *Proc. SPIE* **11840**, 118400H (2021).
- [5] Kimura, K., Sun, M., Ueda, R., Wu, Y., Pan, H., and Momose, A., "High-energy x-ray phase tomography using grating interferometer with structured anode x-ray source," *Proc. SPIE* **11840**, 118400K (2021).
- [6] Hornberger, B., and Kasahara, J., "A compact light source for high-throughput x-ray tomography applications," *Proc. SPIE* **11840**, 118400J (2021).
- [7] Korobenkov, M., and Narikovich, A., "Micro-computed tomography-based characterization of b4c-c composite for x-ray optics," *Proc. SPIE* **11840**, 118401C (2021).
- [8] Marathe, S., Ziesche, R., Das, G., Schroeder, S., Baird, E., and Rau, C., "High-speed grating interferometry," *Proc. SPIE* **11840**, 118400L (2021).
- [9] Rau, C., Marathe, S., Bodey, A., Storm, M., Batey, D., Cipiccia, S., Li, P., and Ziesche, R., "High-throughput micro and nano-tomography," *Proc. SPIE* **11840**, 118401E (2021).
- [10] Thiry, M., Beckmann, F., Hammel, J., Moosmann, J., and Wilde, F., "Brilliant light for materials science: Industrial applications of the high energy microtomography at beamline HEMS/P07 at PETRA III," *Proc. SPIE* **11840**, 118400V (2021).
- [11] Riedel, M., Gustschin, A., Ushakov, L., Noichl, W., Taphorn, K., Busse, M., Beckmann, F., Hammel, J., Moosmann, J., Thibault, P., and Herzen, J., "High-resolution quantitative phase-contrast x-ray imaging for biomedical samples at PETRA III," *Proc. SPIE* **11840**, 118400W (2021).
- [12] Beckmann, F., Wilde, F., Hammel, J., Moosmann, J., Greving, I., Lottermoser, L., Riedel, M., and Thiry, M., "Multi-scale microtomography using synchrotron radiation at beamlines P05/PETRA III and P07/PETRA III," *Proc. SPIE* **11840**, 118400U (2021).
- [13] Shaker, K., Saladino, G. M., Vogt, C., Katsu-Jimenéz, Y., Brodin, B., Kuiper, R., Andersson, K., Li, Y., Larsson, J., Svenda, M., Rodriguez-Garcia, A., Toprak, M., Arsenian-Henriksson, M., and Hertz, H., "Laboratory x-ray fluorescence computed tomography for in vivo preclinical imaging," *Proc. SPIE* **11840**, 118400Y (2021).
- [14] Saladino, G. M., Vogt, C., Li, Y., Shaker, K., Brodin, B., Svenda, M., Hertz, H. M., and Toprak, M. S., "Optical and X-ray Fluorescent Nanoparticles for Dual Mode Bioimaging," *ACS Nano* **15**(3), 5077-5085 (2021).
- [15] Andrew, M., Omlor, L., Andreyev, A., Sanapala, R., and Samadi Khoshkhoo, M., "New technologies for x-ray microscopy: phase correction and fully automated deep learning based tomographic reconstruction," *Proc. SPIE* **11840**, 118400I (2021).
- [16] Zhang, Q., Ye, X., and Chen, Y., "Nonsmooth nonconvex LDCT image reconstruction via learned descent algorithm," *Proc. SPIE* **11840**, 1184013 (2021).
- [17] Grewar, M., Myers, G., and Kingston, A., "Least-squares and maximum-likelihood in XCT," *Proc. SPIE* **11840**, 1184014 (2021).
- [18] Niu, C., Li, M., and Wang, G., "Multi-window learning for metal artifact reduction," *Proc. SPIE* **11840**, 1184015 (2021).
- [19] Li, M., Cong, W., and Wang, G., "High-resolution interior tomography with a deep neural network trained on a low-resolution dataset," *Proc. SPIE* **11840**, 1184018 (2021).

- [20] Tanner, C., Rodgers, G., Schulz, G., Osterwalder, M., Mani-Caplazi, G., Hotz, G., Scheel, M., Weitkamp, T., and Müller, B., "Extended-field synchrotron microtomography for non-destructive analysis of incremental lines in archeological human teeth cementum," *SPIE Optical Engineering + Applications* **11840**, 1184019 (2021).
- [21] Davis, G., "Simulation of polychromatic x-ray attenuation to validate and improve two-dimensional beam-hardening correction," *Proc. SPIE* **11840**, 118401A (2021).
- [22] Schaff, F., Morgan, K., Paganin, D., and Kitchen, M., "Spectral propagation-based x-ray phase-contrast imaging," *Proc. SPIE* **11840**, 118400C (2021).
- [23] Wiedeman, C., Cong, W., and Wang, G., "Simultaneous electron density and attenuation coefficient reconstruction," *Proc. SPIE* **11840**, 118400D (2021).
- [24] Yang, Q., Chakraborty, N., Lakshtanov, D., Sheppard, A., and Kingston, A., "Density estimation in XCT using the Alvarez-Makovski model," *proc. SPIE* **11840**, 118400E (2021).
- [25] Ueda, R., Hashimoto, K., Takano, H., Cai, M., and Momose, A., "Reconstruction method for grating-based x-ray phase tomographic microscope," *Proc. SPIE* **11840**, 118400F (2021).
- [26] Alloo, S., Paganin, D., Morgan, K., Kitchen, M., Stevenson, A., Mayo, S., Li, H., Kennedy, B., Maksimenko, A., Bowden, J., and Pavlov, K., "Speckle-based x-ray dark-field tomography of an attenuating object," *Proc. SPIE* **11840**, 118400G (2021).
- [27] Ammann, R., Tanner, C., Schulz, G., Osmani, B., Nalabothu, P., Töpper, T., and Müller, B., "Three-dimensional analysis of aligner gaps and thickness distributions using advanced laboratory-based hard x-ray tomography," *Proc. SPIE* **11840**, (2021).
- [28] Cooley, V., Stock, S., Guise, W., Verma, A., Wald, T., Klein, O., and Joester, D., "Semantic segmentation of mouse jaws using convolutional neural networks," *Proc. SPIE* **11840**, 1184009 (2021).
- [29] Lindgren, E., and Zach, C., "Analysis of industrial X-ray computed tomography data with deep neural networks," *Proc. SPIE* **11840**, 118400B (2021).
- [30] Schulz, G., Nicklisch, N., Rojo Guerra, M., Müller, B., and Alt, K., "Prehistoric beaten-copper cranium," *Proc. SPIE* **11840**, 1184006 (2021).
- [31] Nelson, A., "Developments in the use of x-ray tomography for the study of ancient mummies," *Proc. SPIE* **11840**, 1184007 (2021).
- [32] Romell, J., Jie, V. W., Miettinen, A., Baird, E., and Hertz, H., "Stain-free virtual histology of *Bombus terrestris* compound eyes by laboratory phase-contrast nano-CT," *Proc. SPIE* **11840**, 118400O (2021).
- [33] Romell, J., Jie, V. W., Miettinen, A., Baird, E., and Hertz, H. M., "Laboratory phase-contrast nanotomography of unstained *Bombus terrestris* compound eyes," *Journal of Microscopy* **283**(1), 29-40 (2021).
- [34] Mills, D., and Boyde, A., "Correlative light microscopy and x-ray microtomography of ground sections of mineralised tissues," *Proc. SPIE* **11840**, 1184010 (2021).
- [35] Stock, S. R., Morse, P., Stock, M., James, K., Natanson, L., Chen, H., Shevchenko, P., Maxey, E., Antipova, O., and Park, J., "3D tomography of shark vertebrae via energy dispersive diffraction," *Proc. SPIE* **11840**, 118400N (2021).
- [36] Iskhakova, K., Wieland, D. C. F., Zeller-Plumhoff, B., and Willumeit-Römer, R., "X-ray diffraction tomography as a tool to study the influence of biodegradable metal implant on the bone in 3D," *Proc. SPIE* **11840**, 118400M (2021).
- [37] Eckermann, M., Ruhwedel, T., Möbius, W., and Salditt, T., "Towards correlative imaging of neuronal tissue by phase-contrast x-ray tomography and SEM," *Proc. SPIE* **11840**, 1184005 (2021).
- [38] Rodgers, G., Tanner, C., Schulz, G., Migga, A., Weitkamp, T., Kuo, W., Scheel, M., Osterwalder, M., Kurtcuoglu, V., and Müller, B., "Impact of fixation and paraffin embedding on mouse brain morphology: a synchrotron radiation-based tomography study," *Proc. SPIE* **11840**, 118400P (2021).

- [39] Rodgers, G., Kuo, W., Schulz, G., Scheel, M., Migga, A., Bikis, C., Tanner, C., Kurtcuoglu, V., Weitkamp, T., and Müller, B., "Virtual histology of an entire mouse brain from formalin fixation to paraffin embedding. Part 2: Volumetric strain fields and local contrast changes," *J Neurosci Methods* **365**, 109385 (2022).
- [40] Rodgers, G., Kuo, W., Schulz, G., Scheel, M., Migga, A., Bikis, C., Tanner, C., Kurtcuoglu, V., Weitkamp, T., and Müller, B., "Virtual histology of an entire mouse brain from formalin fixation to paraffin embedding. Part 1: Data acquisition, anatomical feature segmentation, tracking global volume and density changes," *J Neurosci Methods* **364**, 109354 (2021).
- [41] Twengström, W., Fernandez Moro, C., Romell, J., Larsson, J., Sparrelid, E., Björnstedt, M., and Hertz, H., "Laboratory phase-contrast CT for 3D tumor resection margin assessment," *Proc. SPIE* **11840**, 118400Q (2021).
- [42] Roche i Morgo, O., Massimi, L., Suaris, T., Endrizzi, M., Munro, P. R., Savvidis, S., Havariyoun, G., Hawker, P. M. S., Astolfo, A., Larkin, O., Nelan, R., Jones, J. L., Pelt, D., Bate, D., Olivo, A., and Hagen, C., "Exploring the potential of cycloidal computed tomography for advancing intraoperative specimen imaging," *Proc. SPIE* **11840**, 118400R (2021).
- [43] Arhatari, B., Nesterets, Y., Taba, S., Maksimenko, A., Hall, C., Stevenson, A., Häsermann, D., Lewis, S., Dimmock, M., Thompson, D., Mayo, S., Quiney, H., Gureyev, T., and Brennan, P., "X-ray phase-contrast computed tomography for full breast mastectomy imaging at the Australian Synchrotron," *Proc. SPIE* **11840**, 1184012 (2021).
- [44] Zdora, M.-C., Thibault, P., and Zanette, I., "X-ray speckle-based phase-contrast imaging: principle and applications," *Proc. SPIE* **11840**, 118400S (2021).
- [45] Zhang, Y., Chen, H., Xia, W., Chen, Y., Liu, B., Liu, Y., Sun, H., and Zhou, J., "Dual-domain reconstruction network for sparse-view CT," *Proc. SPIE* **11840**, 1184016 (2021).
- [46] Migga, A., Schulz, G., Rodgers, G., Osterwalder, M., Tanner, C., Blank, H., Jerjen, I., Salmon, P., Twengström, W., Scheel, M., Weitkamp, T., Schlepütz, C., Bolten, J., Huwyler, J., Hotz, G., Madduri, S., and Müller, B., "Laboratory-based phase and absorption tomography for micro-imaging of annual layers in human tooth cementum, paraffin-embedded nerve and zebrafish embryo," *Proc. SPIE* **11840**, 118400T (2021).